nature medicine

ASC-J9 ameliorates spinal and bulbar muscular atrophy phenotype via degradation of androgen receptor

Zhiming Yang[1,2,7], Yu-Jia Chang[1,3,7], I-Chen Yu[1], Shuyuan Yeh[1], Cheng-Chia Wu[1,3], Hiroshi Miyamoto[1], Diane E Merry[4], Gen Sobue[5], Lu-Min Chen[1,6], Shu-Shi Chang[1,6] & Chawnshang Chang[1]

Motor neuron degeneration resulting from the aggregation of the androgen receptor with an expanded polyglutamine tract (AR-polyQ) has been linked to the development of spinal and bulbar muscular atrophy (SBMA or Kennedy disease). Here we report that adding 5-hydroxy-1,7-bis(3,4-dimethoxyphenyl)-1,4,6-heptatrien-3-one (ASC-J9) disrupts the interaction between AR and its coregulators, and also increases cell survival by decreasing AR-polyQ nuclear aggregation and increasing AR-polyQ degradation in cultured cells. Intraperitoneal injection of ASC-J9 into AR-polyQ transgenic SBMA mice markedly improved disease symptoms, as seen by a reduction in muscular atrophy. Notably, unlike previous approaches in which surgical or chemical castration was used to reduce SBMA symptoms, ASC-J9 treatment ameliorated SBMA symptoms by decreasing AR-97Q aggregation and increasing VEGF164 expression with little change of serum testosterone. Moreover, mice treated with ASC-J9 retained normal sexual function and fertility. Collectively, our results point to a better therapeutic and preventative approach to treating SBMA, by disrupting the interaction between AR and AR coregulators.

X-linked spinal and bulbar muscular atrophy (SBMA or Kennedy disease) is an inherited neurodegenerative disorder caused by the expansion of the polyglutamine tract of the androgen receptor (AR-polyQ)[1–3]. The length of the AR-polyQ tract is inversely correlated with the age of SBMA onset[1–3]. The effects of the disease are only seen in males, as female carriers are usually asymptomatic. Characteristics of SBMA include proximal muscular atrophy, weakness, contraction fasciculation and bulbar involvement[4]. The nuclear inclusions containing AR-polyQ in the residual motor neurons of the brain stem, spinal cord and other visceral organs[5] are considered to be relevant to the pathophysiology of this disease[6].

In normal individuals, AR (ref. 7), upon activation by androgen, functions as a transcriptional regulator[8] by interacting with a variety of coregulatory proteins[9,10]. In motor neurons, one of the key AR coregulators is the cAMP response element–binding protein (CREB)-binding protein (CBP)[11], which controls the expression of the gene encoding VEGF164 among other genes.

Several mechanisms have been proposed to explain the pathogenesis of SBMA and to suggest potential targets for medical intervention. These mechanisms, which are not necessarily mutually exclusive, include transcriptional deregulation[12], aggregate formation[11,13], proteolysis of causative proteins[14,15], transglutaminase activation[16] and mitochondrial deficits[17]. Transcriptional disturbance, for example through the sequestration of CBP by AR-polyQ aggregates, seems to be one of the most likely causes for the pathogenesis of SBMA. This notion is further supported by the fact that transcriptional deregulation occurs in polyQ-related diseases[18]. Consistent with this idea, manipulations such as chemical or surgical castration, which reduce the level of AR-97Q aggregates[19–21], as well as the administration of a histone deacetylase inhibitor, which restores CBP-mediated transcription, effectively treat SBMA in mice[20]. However, the severe side effects caused by castration, including loss of libido, impotence, osteoporosis and fatigue, and the toxicity of histone deacetylase inhibitors make these approaches unsuitable therapeutic strategies for treating SBMA in men.

A compound that disrupts aggregates comprised of AR-polyQ and various coregulators could have potential therapeutic benefits for two complementary reasons. First, such a compound could increase the level of transcriptionally active coregulators, including CBP, by releasing them from the nonproductive interaction with AR-polyQ. Second, disrupting the aggregates might render the released AR-polyQ more vulnerable to degradation, thereby reducing its toxic effect.

We screened natural products and their derivatives for the disruption of normal AR and its coregulators, and found that 5–hydroxy-1,7-bis(3,4-dimethoxyphenyl)-1,4,6-heptatrien-3-one (ASC-J9) can substantially promote the dissociation of AR and ARA70 (ref. 22). Moreover, we discovered that treatment of prostate cancer cells with ASC-J9 led to decreased AR transactivation, resulting in the suppression of AR-mediated cell proliferation[22]. Using a SBMA PC12/AR-112Q cell line[23] and a SBMA/AR-97Q line of transgenic mice[5] as models, we found that ASC-J9 ameliorated SBMA symptoms with little influence on the concentration of circulating testosterone.

[1]George Whipple Lab for Cancer Research, Departments of Pathology, Urology, and Radiation Oncology, and The Cancer Center, University of Rochester Medical Center, Rochester, New York 14642, USA. [2]Zhejiang University and 2nd Hospital, Hangzhou 310009, China. [3]Taipei Medical University and Hospital, Taipei 110, Taiwan. [4]Thomas Jefferson University, Philadelphia, Pennsylvania 19107, USA. [5]Nagoya University, Nagoya 466-8550, Japan. [6]China Medical University and Hospital, Taichung 404, Taiwan. [7]These authors contributed equally to this work. Correspondence should be addressed to C.C. (chang@URMC.rochester.edu).

Received 10 March 2006; accepted 16 January 2007; published online 4 March 2007; doi:10.1038/nm1547

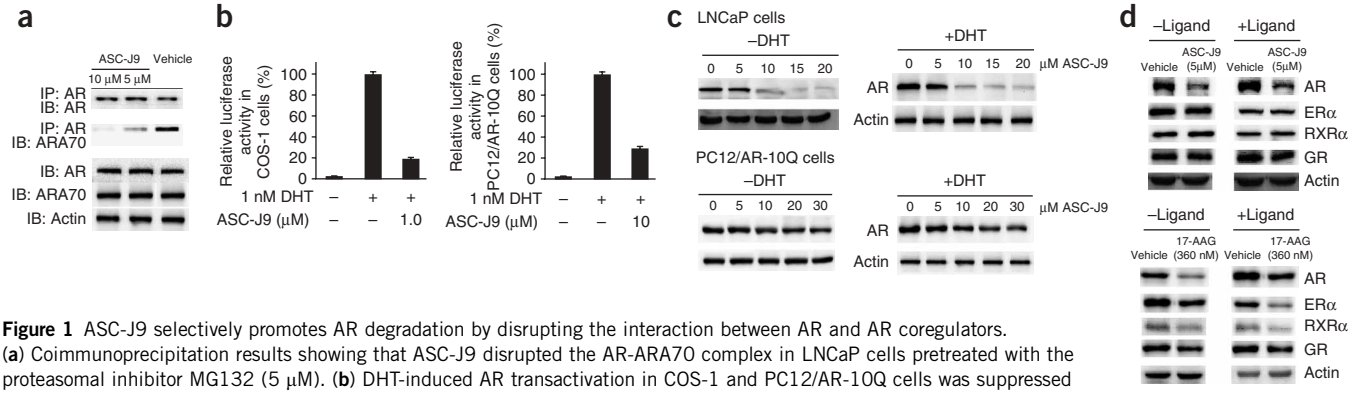

Figure 1 ASC-J9 selectively promotes AR degradation by disrupting the interaction between AR and AR coregulators. (**a**) Coimmunoprecipitation results showing that ASC-J9 disrupted the AR-ARA70 complex in LNCaP cells pretreated with the proteasomal inhibitor MG132 (5 μM). (**b**) DHT-induced AR transactivation in COS-1 and PC12/AR-10Q cells was suppressed after ASC-J9 treatment, as assessed by (ARE)4-LUC reporter assay. (**c**) The steady-state level of AR protein in LNCaP and PC12/AR-10Q cells from western blot assays indicated that the AR signal decreased substantially (in a dose-dependent manner) after treatment with ASC-J9. (**d**) ASC-J9 selectively decreased the steady-state level of AR protein, in the absence and the presence of ligand. In contrast, 17-AAG treatment decreased the steady-state level of all four ligand-activated nuclear receptors (AR, ERα, GR and RXRα), both in the absence and in the presence of the specific ligand.

Moreover, the SBMA mice showed normal sexual activity and improved fertility, suggesting that this strategy might provide a better approach to treating SBMA in men.

RESULTS

ASC-J9 selectively promotes AR degradation

To test our hypothesis that disrupting the interaction between AR and AR-associated proteins is an improved strategy for battling SBMA, we first used a coimmunoprecipitation assay in cultured prostate cancer LNCaP cells, which demonstrated that ASC-J9 promotes the dissociation between AR and its coregulator ARA70 (**Fig. 1a**). We then found that, in COS-1 cells, ASC-J9–induced dissociation between AR and ARA70 led to suppression of AR transactivation (**Fig. 1b**). Similar suppression effects also occurred when we replaced COS-1 cells with PC12/AR-10Q cells (**Fig. 1b**).

To determine whether AR degrades more rapidly when freed of its association with coregulators, we measured the steady-state level of AR protein after the administration of different doses of ASC-J9 in LNCaP and PC12/AR-10Q cells. ASC-J9 treatment decreased the steady-state level of AR protein in the absence and presence of the hormone dihydrotestosterone (DHT), suggesting that ASC-J9 might promote AR protein degradation by disrupting the interaction of AR with AR coregulators (**Fig. 1c**). As the interaction between AR and ARA70 is relatively selective[9], we expected that the degradation of AR by ASC-J9 would also be selective. Whereas ASC-J9 promoted the degradation of AR, it had little effect on other members of the family of ligand-activated nuclear receptors, such as glucocorticoid receptor (GR), estrogen receptor-α (ERα) and retinoid X receptor-α RXRα (**Fig. 1d**). In contrast, the hsp90 inhibitor 17-allylamino-17-demethoxygeldanamycin (17-AAG), which uncouples the interaction between hsp90 and members of this family, unselectively promoted the degradation of AR as well as GR, ERα and RXRα.

Collectively, the results demonstrated that ASC-J9, but not 17-AAG, classic antiandrogen hydroxyflutamide (HF) or curcumin (**Fig. 1d** and **Supplementary Fig. 1** online), can selectively promote AR degradation, which might be secondary to disrupting the interaction between AR and AR coregulators, which results in the suppression of AR transactivation.

ASC-J9 reduces the AR aggregated AR-112Q in cells

The aggregation of AR-polyQ in the nucleus, which is toxic to motor neurons, has been linked to the pathogenesis of SBMA (ref. 11). We tested PC12 cells stably transfected with inducible AR-112Q (PC12/AR-112Q) in a model that mimics the nuclear aggregation present in SBMA (ref. 23) to see whether ASC-J9 can reduce the pathogenesis of SBMA. We found that AR-112Q localized in the cytoplasm in the

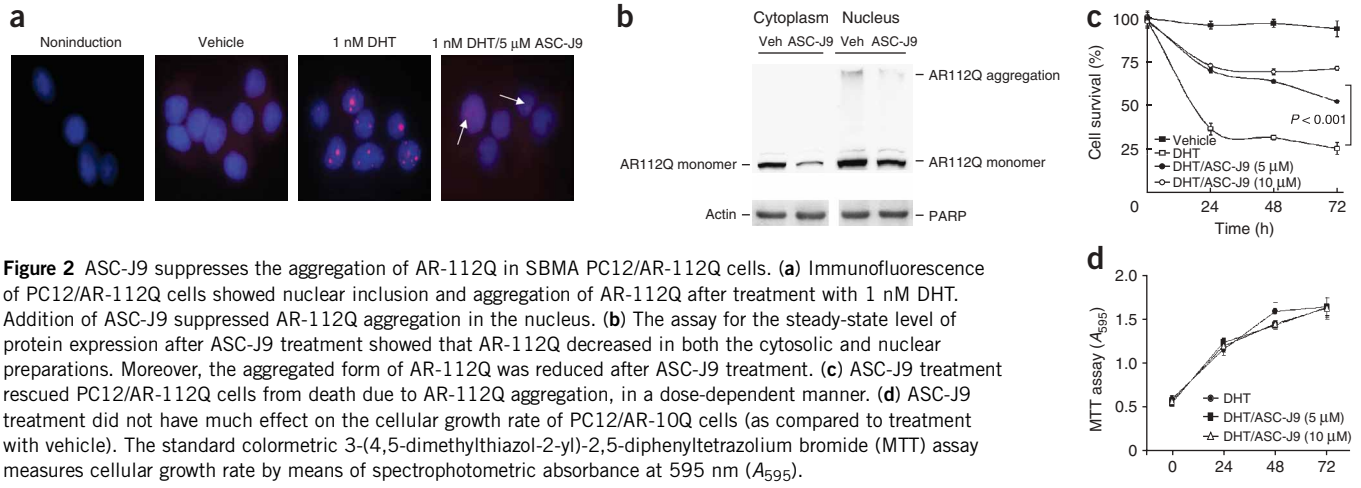

Figure 2 ASC-J9 suppresses the aggregation of AR-112Q in SBMA PC12/AR-112Q cells. (**a**) Immunofluorescence of PC12/AR-112Q cells showed nuclear inclusion and aggregation of AR-112Q after treatment with 1 nM DHT. Addition of ASC-J9 suppressed AR-112Q aggregation in the nucleus. (**b**) The assay for the steady-state level of protein expression after ASC-J9 treatment showed that AR-112Q decreased in both the cytosolic and nuclear preparations. Moreover, the aggregated form of AR-112Q was reduced after ASC-J9 treatment. (**c**) ASC-J9 treatment rescued PC12/AR-112Q cells from death due to AR-112Q aggregation, in a dose-dependent manner. (**d**) ASC-J9 treatment did not have much effect on the cellular growth rate of PC12/AR-10Q cells (as compared to treatment with vehicle). The standard colormetric 3-(4,5-dimethylthiazol-2-yl)-2,5-diphenyltetrazolium bromide (MTT) assay measures cellular growth rate by means of spectrophotometric absorbance at 595 nm (A_{595}).

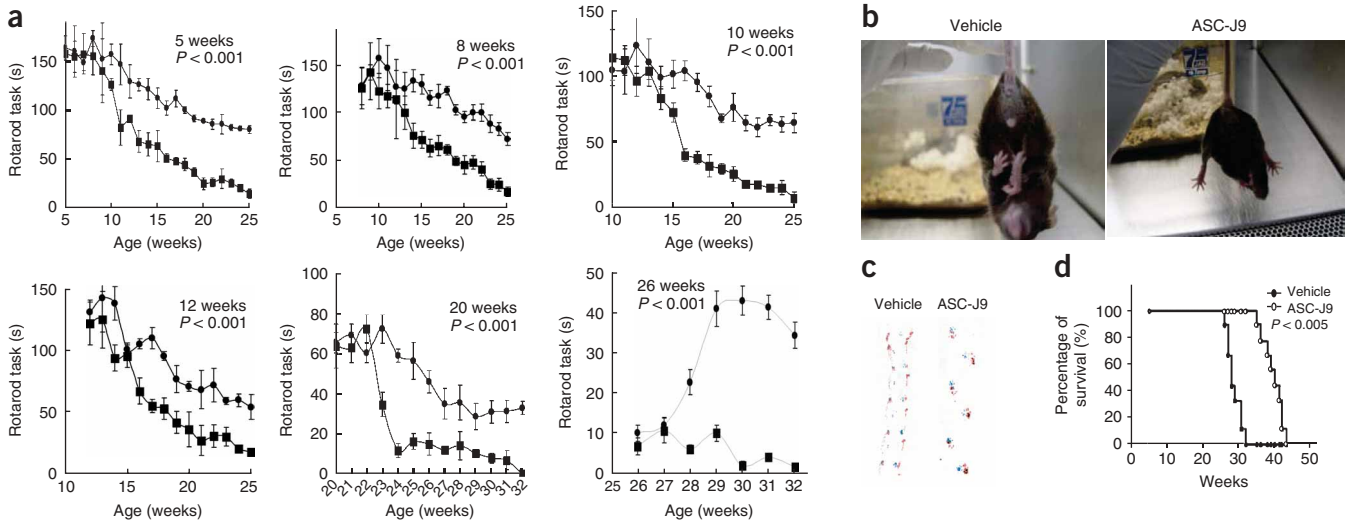

Figure 3 Effects of ASC-J9 (50 mg/kg every 48 h) on SBMA symptoms in male SBMA mice. (**a**) Performance of mice of different ages on the rotarod tasks ($n = 6$ in each group). Mice treated with ASC-J9 showed noticeable improvement even when the treatment started as late as 26 weeks after the onset of SBMA phenotype. (**b**–**d**) SBMA mice were treated with vehicle or ASC-J9 starting at 5 weeks, and were examined at 15 weeks. With ASC-J9, phenotypic clasping behavior was ameliorated (**b**), footprint patterns were normal (**c**) and the survival rate had improved (**d**) ($n = 9$ mice in each group). In **c**, front paws are in blue and hind paws in red.

absence of DHT, and addition of 1 nM DHT resulted in the translocation of AR-112Q into the nucleus and subsequent formation of aggregates (**Fig. 2a**). Notably, addition of 5 μM ASC-J9 substantially suppressed the aggregate formation, with little AR-112Q detected in the nucleus (**Fig. 2a**). Western blotting analysis also showed that ASC-J9 treatment promoted the degradation and reduced the amount of aggregated AR-112Q protein in the nucleus (**Fig. 2b**).

In addition, PC12 cell death induced by AR-112Q nuclear aggregation was rescued by the addition of ASC-J9 in a dose-dependent manner (**Fig. 2c**), with little influence on the proliferation of PC12/AR-10Q cells (**Fig. 2d**). Collectively, these results demonstrated that ASC-J9 might reduce cytotoxicity by suppressing the aggregation of AR-112Q in the nucleus and increasing its degradation in the PC12/AR-112Q cells, with little effect on the PC12/AR-10Q cells.

ASC-J9 rescues the SBMA symptoms in AR-97Q mice

We further examined the *in vivo* effects of ASC-J9 in SBMA mice with transgenic AR-97Q (ref. 5). Every other day, we injected male SBMA mice intraperitoneally with ASC-J9 in corn oil at the effective dose of 50 mg per kg body weight, and assessed their motor impairment by testing rotarod activity weekly. We found that the motor impairments were substantially improved in SBMA mice treated with ASC-J9, regardless of whether treatment was started early (at 5 weeks of age) or later (at 26 weeks) (**Fig. 3a**). This observation suggests that ASC-J9 treatment substantially delays the onset and symptomatic progression of motor impairment, which usually appears at 10 weeks. We also found that cage activity increased in SBMA mice treated with ASC-J9 (**Supplementary Video 1** online). The SBMA symptoms of gait disturbance, including severe dragging of hind limbs and erratic footprinting patterns, markedly declined in ASC-J9–treated SBMA mice, suggesting that ASC-J9 treatment can substantially ameliorate the SBMA symptoms in these mice (**Fig. 3b,c**). Notably, ASC-J9 treatment prolonged the lives of these mice, from an average of 28 weeks to 39 weeks (**Fig. 3d**).

Improved sexual functions in SBMA mice treated with ASC-J9

SBMA patients might be reluctant to undergo the helpful but aggressive treatment of surgical or chemical castration because such treatments suppress serum testosterone levels, leading to a loss of normal sexual genital functions and fertility. Notably, we found that ASC-J9–treated SBMA mice had relatively normal serum testosterone concentrations (**Fig. 4a**). Sexual activity, as judged by vaginal plug numbers in female mice caged with the treated males, and fertility, as judged by both pup numbers and litter numbers, were substantially improved during 4 weeks of fertility tests (**Fig. 4b**).

These results demonstrated that there was little adverse influence on serum testosterone and that sexual genital functions and fertility were in fact improved in SBMA mice treated with ASC-J9.

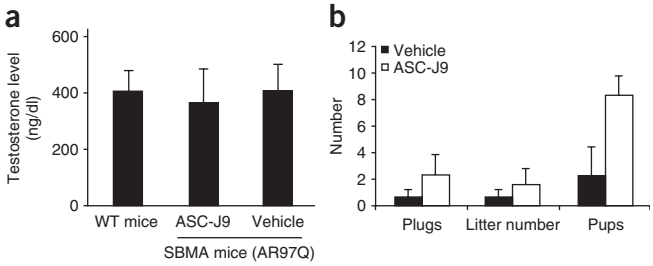

Figure 4 Effect of ASC-J9 (50 mg/kg every 48h) on the fertility and testosterone level of male SBMA mice. We began treatment of SBMA mice at 5 weeks of age. (**a**) We took blood samples from wild-type (WT) and vehicle- or ASC-J9–treated SBMA mice at 20 weeks of age ($n = 9$ mice in each group), and measured serum testosterone levels using an ELISA kit. We found little difference between vehicle- and ASC-J9–treated mice in terms of serum testosterone levels. (**b**) Fertility tests performed on 13-week-old SBMA mice ($n = 4$ mice in each group) showed increased sexual activity following ASC-J9 treatment (compared to vehicle treatment).

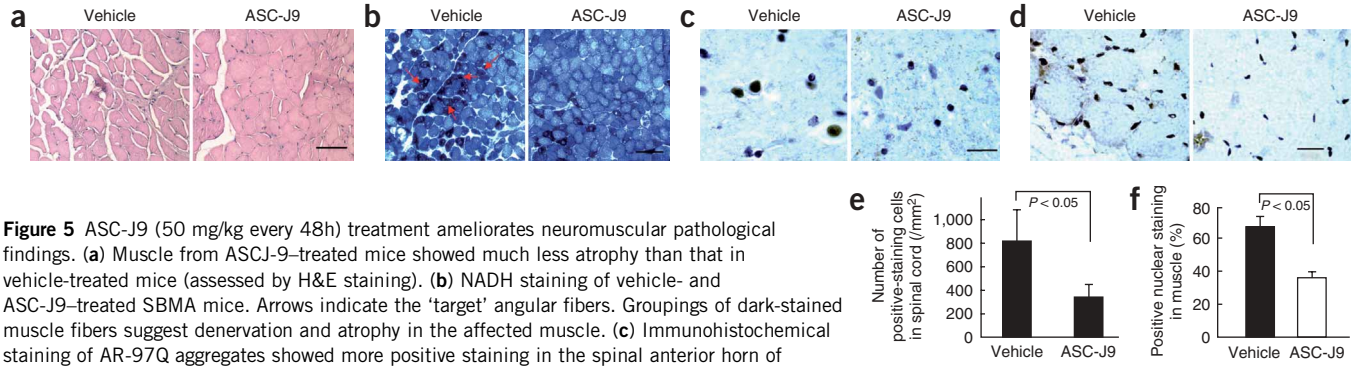

Figure 5 ASC-J9 (50 mg/kg every 48h) treatment ameliorates neuromuscular pathological findings. (**a**) Muscle from ASCJ-9–treated mice showed much less atrophy than that in vehicle-treated mice (assessed by H&E staining). (**b**) NADH staining of vehicle- and ASC-J9–treated SBMA mice. Arrows indicate the 'target' angular fibers. Groupings of dark-stained muscle fibers suggest denervation and atrophy in the affected muscle. (**c**) Immunohistochemical staining of AR-97Q aggregates showed more positive staining in the spinal anterior horn of vehicle-treated mice than in ASC-J9–treated mice. (**d**) Muscle fibers of SBMA mice treated with ASC-J9 showed much less aggregation of AR-112Q than the muscle fibers from vehicle-treated SBMA mice. (**e**,**f**) There was approximately 50% reduction in AR-aggregated positive-staining cells in the spinal cord and the muscle fibers after ASC-J9 treatment compared with vehicle treatment. Scale bars: 100 μm in **a** and **b**, 20 μm in **c** and **d**.

ASC-J9 reverses muscular atrophy and restores VEGF expression

Hematoxylin and eosin staining showed that ASC-J9 treatment substantially reduced muscular atrophy compared to vehicle treatment (**Fig. 5a**). By using nicotinamide adenine dinucleotide (NADH) to stain muscle, we also found that the groupings of muscle fibers were markedly altered in the ASC-J9–treated mice (**Fig. 5b**). There were more groupings of ankylated muscle fibers, suggesting the denervation and atrophy of muscle fibers, in vehicle-treated mice than in ASC-J9–treated mice (**Fig. 5b**). Immunohistochemical staining using an antibody to AR, N20, showed the intranuclear aggregation of AR-97Q in spinal cord motor neurons and skeletal muscle cells (**Fig. 5c**,**d**). Also, the intranuclear AR-97Q aggregation in spinal cord neurons and muscle cells was significantly lower (by almost 50%) in the ASC-J9–treated mice than in the vehicle-treated mice (**Fig. 5e**,**f**).

Motor neuron survival and proper function requires VEGF164 expression. Previous studies have suggested that aggregated AR-97Q might associate abnormally with CBP, resulting in the disruption of CBP-mediated VEGF164 expression[24]. By examining coimmunoprecipitation in PC12/AR-112Q and PC12/AR-Q10 cells, we found that ASC-J9 dose-dependently disrupted the interaction between AR-112Q and CBP in PC12/AR-112Q cells but had little influence in PC12/AR-10Q cells (**Fig. 6a**). Releasing CBP from its interaction with AR-112Q in PC12/AR-112Q cells was associated with the induction of VEGF164 expression (**Fig. 6b**).

We further confirmed this finding by showing a significant increase (from 20% to 90%) in the expression of mRNA for VEGF164 in the spinal cord of SBMA mice following ASC-J9 treatment (**Fig. 6c**). Moreover, the ELISA assay to detect the levels of VEGF protein in the spinal cord of these mice also demonstrated a significant increase of VEGF expression after ASC-J9 treatment (**Fig. 6d**). These results do not formally prove that ASC-J9 ameliorates SBMA symptoms by restoring VEGF164 expression, but they are consistent with this idea.

DISCUSSION

It has been shown that one of hsp90's associated proteins, AR, can be degraded when the interaction between hsp90 and its associated proteins is disrupted by using the hsp90 inhibitor 17-AAG. This degradation reduces the longer AR-97Q nuclear aggregates in SBMA mice[25]. However, 17-AAG also disrupts the interaction between hsp90 and many other proteins, including GR, ERα and RXRα (**Fig. 1d**), and Her2, Her3 receptor tyrosine kinase, Erk1/2 and Rb (refs. 25–30), rendering them more susceptible to degradation. Recent reports have clearly documented that common adverse reactions to 17-AAG include anorexia, diarrhea, nausea, fatigue and vomiting, along with the reversible elevation of liver enzymes (in 29.5% of subjects)[31]. This inhibitor also enhances bone metastasis and osteolytic lesions, which

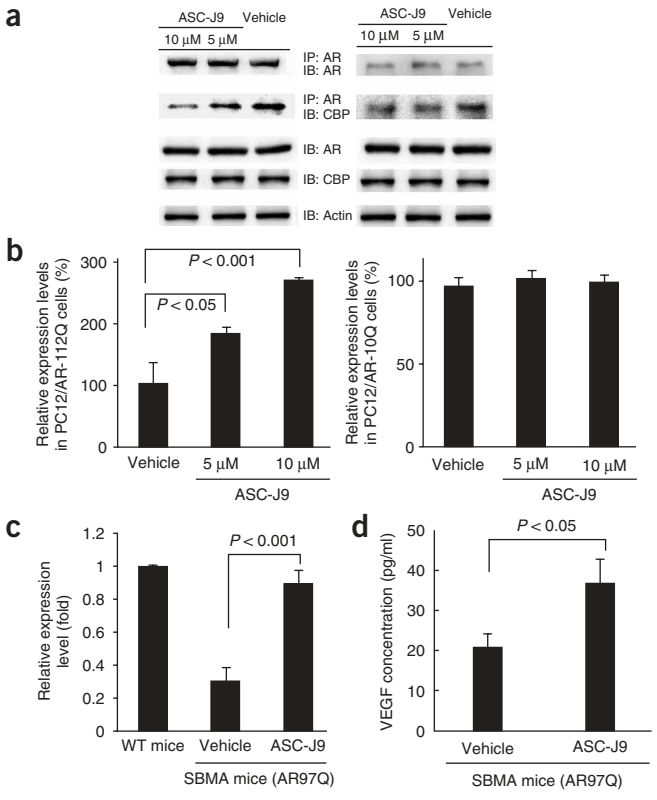

Figure 6 Molecular mechanisms of the effect of ASC-J9 on the SBMA phenotypes. (**a**) Treatment with 5 μM or 10 μM ASC-J9 showed dose-dependent disruption of the interaction between CBP and AR-112Q or AR-10Q in PC12 cells pretreated with the proteasomal inhibitor MG132 (5 μM). (**b**) ASC-J9 treatment increased VEGF164 expression in PC12/AR-112Q cells but had little influence in PC12/AR-10Q cells pretreated with MG132. (**c**) ASC-J9 treatment had a dose-dependent effect on increasing mRNA for VEGF164 in the spinal cord. (**d**) Amounts of VEGF protein from homogenized L5 spinal cords were increased after ASC-J9 treatment.

lead to increased osteolysis and incidence of skeletal tumors[32]. The nonspecific disruption by 17-AAG of the interaction between hsp90 and most of its associated proteins leads to extensive adverse and unwanted side effects, and therefore limits the applicability of 17-AAG in the treatment of SBMA. In contrast, ASC-J9 (at a dose of 50 mg/kg every 48 h for more than 20 weeks) had no obvious toxic effects and did not result in a loss of body weight in mice. Moreover, the sexual genital functions and fertility in these SBMA mice were improved markedly. Together, these positive results of ASC-J9 treatment demonstrate that this new approach—involving the selective disruption of interactions between AR-polyQ and AR coregulators, such as CBP—might offer improved treatment for SBMA. Additional dosage studies of ASC-J9 or its derivatives to investigate how SBMA symptoms may be effectively ameliorated, without toxicity, might lead to treatments that could substantially improve the quality of life of SBMA patients.

METHODS

Therapeutic agent and administration protocol. ASC-J9 from AndroScience was synthesized as described previously[22]. We dissolved it in corn oil and injected it intraperitoneally into mice (50 mg/kg every other day) at various ages until the end of the study. Control mice received DMSO in corn oil only.

ASC-J9 characterization. For the AR degradation study, we treated LNCaP cells with vehicle and 1 nM DHT with or without 5 μM ASC-J9, in RPMI supplemented with 10% charcoal dextran–stripped (CDS) FBS. At selected time intervals, we harvested cells and analyzed AR protein levels by western blotting, quantitated the results by Bio-Rad PDQuest Image software, and normalized densitometric values to actin. We purchased the antibodies for AR (N20), CBP (C-1), ERα (HC-20), GR (P-20), RXRα (D-20), CBP, PARP and actin from Santa Cruz Biotechnology and generated ARA70 antibody as previously described[33].

For the AR-112Q protein steady-state assay, we cultured PC12/AR-112Q cells as described previously[23], in the presence of 10 μg/ml doxycycline for 24 h, and then treated cells with or without 1 nM DHT or 1 nM DHT and 5 μM ASC-J9 for 3 d. We performed the cytosolic and nuclear extraction by FractionPREP™ Cell Fraction System (BioVision) and analyzed the AR-112Q by western blotting.

We performed the protein steady-state assay of AR, GR, ERα and RXRα in response to 5 μM ASC-J9 or 360 nM 17-AAG, on LNCaP cells (AR and RXRα), MCF-7 cells (ERα) and PC3 cells (GR), in the presence or absence of ligand (1 nM DHT for AR, 1 nM E2 for ERα, 1 nM dexamethasone for GR and 1 μM 9-cis-RA for RXRα). We determined the amounts of AR, GR, ERα and RXRα proteins by western blotting and analyzed the interactions between AR-ARA70 complex and AR-CBP complex by coimmunoprecipitation[24,33]. We assayed AR transactivation activity as described previously[34].

Immunofluorescence staining and cell survival. We cultured PC12/AR-112Q cells in two-well Chamber slides (Nalge Nunc) supplemented by DMEM, 10% CDS horse serum and 100 μg/ml nerve growth factor (BD Biosciences), and induced AR-112Q by 10 μg/ml doxycycline (Sigma) for 4 h. Then we treated cells with vehicle, 1 nM DHT, or 1 nm DHT and 5 μM ASC-J9 for 3 d. We stained AR-112Q with N20 antibody and Texas Red–conjugated streptavidin (Vector Laboratories), mounted slides in fluorescent mounting medium containing 4′,6-diamidino-2-phenylindole (DAPI), and observed fluorescent staining using an Olympus fluorescent microscope.

For the cell survival assay, we cultured PC12/AR-112Q and PC12/AR-10Q cells as described previously[23] and incubated cells in the presence of 10 μg/ml doxycycline for 24 h. Then we treated cells with vehicle, 5 μM ASC-J9 or 10 μM ASC-J9, along with 1 nM DHT, and determined cell viability using Trypan blue staining at specific time intervals.

SBMA mouse model generation, maintenance, genotyping and motor activity assessment. We generated the AR-97Q SBMA mice as described previously[5]. We performed all animal experiments in accordance with the Guide for the Care and Use of Laboratory Animals of the US National Institutes of Health and with approval from the Department of Laboratory Animal Medicine at the University of Rochester. We assessed rotarod performance weekly using an Economex Rotarod (Colombus Instruments) as described[35], and observed footprints for ASC-J9– or vehicle-treated SBMA mice by dipping their forepaws in water-soluble red paint and hind paws in blue paint. The mice then walked through a narrow tunnel, leaving footprints on a strip of white paper[21].

Serum testosterone and male fertility. We killed SBMA mice receiving ASC-J9 or vehicle treatment at 20 weeks of age, drew 1 ml of blood by cardiocentesis, and assayed serum testosterone with the Coat-A-Count Total Testosterone radioimmunoassay (Diagnostic Products) according to the manufacturer's protocol. We observed the reproductive capacities of ASC-J9 and vehicle-treated SBMA mice by mating one male mouse with two B6 female mice for 1 week checking female mice for vaginal plugs each morning and recording litter sizes on delivery after four successive matings.

Histology and immunohistochemistry. We fixed tissues by 4% paraformaldehyde and embedded them in paraffin. For general histologic inspection, we treated tissue sections with H&E or NADH, and then used an ABC kit (Vector Laboratories) to detect AR immunostaining by an N20 antibody to AR. We performed the assessment of cells with intranuclear aggregated AR-polyQ in the ventral horn of the spinal cord as described previously[36,37]. We expressed the populations of AR-positive cells as the number per square millimeter. We counted AR-positive cells in randomly selected areas from more than 500 muscle fibers and expressed AR-positive cells as the number per 100 muscle fibers.

Quantitative real time RT-PCR. We harvested L5 spinal cords of mice treated with vehicle or ASC-J9 (50 mg/kg every 48 h), extracted total RNA using TRIZOL and reverse transcribed. We subjected 1 μg of total RNA to reverse transcription using Superscript II (Invitrogen), with the primer probe sequences and PCR conditions for VEGF164 as described previously[24]. We performed amplification, detection, and data analysis using a Bio-Rad iCycler system.

ELISA. We obtained total protein lysates by homogenizing tissues in an extraction buffer as described previously[24]. After centrifugation, we analyzed the amount of VEGF protein in the supernatant using ELISA kit (R&D Systems).

Statistical analysis. We analyzed the results by unpaired *t*-tests and log-rank tests for survival rate using Sigmaplot software. *P*-values less than 0.05 were considered to be statistically significant.

Note: Supplementary information is available on the Nature Medicine website.

ACKNOWLEDGMENTS

We thank K. Wolf for help in editing the manuscript. This work was supported by US National Institutes of Health grant DK067686 and the George Whipple Professorship Endowment.

COMPETING INTERESTS STATEMENT

The authors declare competing financial interests (see the *Nature Medicine* website for details).

Published online at http://www.nature.com/naturemedicine
Reprints and permissions information is available online at http://npg.nature.com/reprintsandpermissions

1. Kennedy, W.R., Alter, M. & Sung, J.H. Progressive proximal spinal and bulbar muscular atrophy of late onset: a sex-linked recessive trait. *Neurology* **50**, 583–593 (1998).
2. La Spada, A.R., Wilson, E.M., Lubahn, D.B., Harding, A.E. & Fischbeck, K.H. Androgen receptor gene mutations in X-linked spinal and bulbar muscular atrophy. *Nature* **352**, 77–79 (1991).
3. Ringel, S.P., Lava, N.S., Treihaft, M.M., Lubs, M.L. & Lubs, H.A. Late-onset X-linked recessive spinal and bulbar muscular atrophy. *Muscle Nerve* **1**, 297–307 (1978).
4. Sobue, G. *et al.* X-linked recessive bulbospinal neuronopathy. A clinicopathological study. *Brain* **112**, 209–232 (1989).
5. Katsuno, M. *et al.* Testosterone reduction prevents phenotypic expression in a transgenic mouse model of spinal and bulbar muscular atrophy. *Neuron* **35**, 843–854 (2002).
6. Li, M. *et al.* Nuclear inclusions of the androgen receptor protein in spinal and bulbar muscular atrophy. *Ann. Neurol.* **44**, 249–254 (1998).

7. Chang, C.S., Kokontis, J. & Liao, S.T. Molecular cloning of human and rat complementary DNA encoding androgen receptors. *Science* **240**, 324–326 (1988).
8. Heinlein, C.A. & Chang, C. Androgen receptor in prostate cancer. *Endocr. Rev.* **25**, 276–308 (2004).
9. Yeh, S. & Chang, C. Cloning and characterization of a specific coactivator, ARA70, for the androgen receptor in human prostate cells. *Proc. Natl. Acad. Sci. USA* **93**, 5517–5521 (1996).
10. Heinlein, C.A. & Chang, C. Androgen receptor (AR) coregulators: an overview. *Endocr. Rev.* **23**, 175–200 (2002).
11. McCampbell, A. & Fischbeck, K.H. Polyglutamine and CBP: fatal attraction? *Nat. Med.* **7**, 528–530 (2001).
12. Sherman, M.Y. & Goldberg, A.L. Cellular defenses against unfolded proteins: a cell biologist thinks about neurodegenerative diseases. *Neuron* **29**, 15–32 (2001).
13. Ross, C.A. Polyglutamine pathogenesis: emergence of unifying mechanisms for Huntington's disease and related disorders. *Neuron* **35**, 819–822 (2002).
14. Merry, D.E., Kobayashi, Y., Bailey, C.K., Taye, A.A. & Fischbeck, K.H. Cleavage, aggregation and toxicity of the expanded androgen receptor in spinal and bulbar muscular atrophy. *Hum. Mol. Genet.* **7**, 693–701 (1998).
15. Tarlac, V. & Storey, E. Role of proteolysis in polyglutamine disorders. *J. Neurosci. Res.* **74**, 406–416 (2003).
16. Mandrusiak, L.M. *et al.* Transglutaminase potentiates ligand-dependent proteasome dysfunction induced by polyglutamine-expanded androgen receptor. *Hum. Mol. Genet.* **12**, 1497–1506 (2003).
17. Beauchemin, A.M. *et al.* Cytochrome c oxidase subunit Vb interacts with human androgen receptor: a potential mechanism for neurotoxicity in spinobulbar muscular atrophy. *Brain Res. Bull.* **56**, 285–297 (2001).
18. Katsuno, M. & Sobue, G. Polyglutamine diminishes VEGF; passage to motor neuron death? *Neuron* **41**, 677–679 (2004).
19. Katsuno, M. *et al.* Leuprorelin rescues polyglutamine-dependent phenotypes in a transgenic mouse model of spinal and bulbar muscular atrophy. *Nat. Med.* **9**, 768–773 (2003).
20. Minamiyama, M. *et al.* Sodium butyrate ameliorates phenotypic expression in a transgenic mouse model of spinal and bulbar muscular atrophy. *Hum. Mol. Genet.* **13**, 1183–1192 (2004).
21. Chevalier-Larsen, E.S. *et al.* Castration restores function and neurofilament alterations of aged symptomatic males in a transgenic mouse model of spinal and bulbar muscular atrophy. *J. Neurosci.* **24**, 4778–4786 (2004).
22. Ohtsu, H. *et al.* Antitumor agents. 217. Curcumin analogues as novel androgen receptor antagonists with potential as anti-prostate cancer agents. *J. Med. Chem.* **45**, 5037–5042 (2002).
23. Walcott, J.L. & Merry, D.E. Ligand promotes intranuclear inclusions in a novel cell model of spinal and bulbar muscular atrophy. *J. Biol. Chem.* **277**, 50855–50859 (2002).
24. Sopher, B.L. *et al.* Androgen receptor YAC transgenic mice recapitulate SBMA motor neuronopathy and implicate VEGF164 in the motor neuron degeneration. *Neuron* **41**, 687–699 (2004).
25. Waza, M. *et al.* 17-AAG, an Hsp90 inhibitor, ameliorates polyglutamine-mediated motor neuron degeneration. *Nat. Med.* **11**, 1088–1095 (2005).
26. Goetz, M.P., Toft, D.O., Ames, M.M. & Erlichman, C. The Hsp90 chaperone complex as a novel target for cancer therapy. *Ann. Oncol.* **14**, 1169–1176 (2003).
27. Solit, D.B. *et al.* 17-Allylamino-17-demethoxygeldanamycin induces the degradation of androgen receptor and HER-2/neu and inhibits the growth of prostate cancer xenografts. *Clin. Cancer Res.* **8**, 986–993 (2002).
28. Barent, R.L. *et al.* Analysis of FKBP51/FKBP52 chimeras and mutants for Hsp90 binding and association with progesterone receptor complexes. *Mol. Endocrinol.* **12**, 342–354 (1998).
29. Smith, D.F. *et al.* Progesterone receptor structure and function altered by geldanamycin, an hsp90-binding agent. *Mol. Cell. Biol.* **15**, 6804–6812 (1995).
30. Hostein, I., Robertson, D., DiStefano, F., Workman, P. & Clarke, P.A. Inhibition of signal transduction by the Hsp90 inhibitor 17-allylamino-17-demethoxygeldanamycin results in cytostasis and apoptosis. *Cancer Res.* **61**, 4003–4009 (2001).
31. Banerji, U. *et al.* Phase I pharmacokinetic and pharmacodynamic study of 17-allylamino, 17-demethoxygeldanamycin in patients with advanced malignancies. *J. Clin. Oncol.* **23**, 4152–4161 (2005).
32. Price, J.T. *et al.* The heat shock protein 90 inhibitor, 17-allylamino-17-demethoxygeldanamycin, enhances osteoclast formation and potentiates bone metastasis of a human breast cancer cell line. *Cancer Res.* **65**, 4929–4938 (2005).
33. Thin, T.H. *et al.* Mutations in the helix 3 region of the androgen receptor abrogate ARA70 promotion of 17beta-estradiol-induced androgen receptor transactivation. *J. Biol. Chem.* **277**, 36499–36508 (2002).
34. Wang, L. *et al.* Suppression of androgen receptor-mediated transactivation and cell growth by the glycogen synthase kinase 3 beta in prostate cells. *J. Biol. Chem.* **279**, 32444–32452 (2004).
35. Garden, G.A. *et al.* Polyglutamine-expanded ataxin-7 promotes non-cell-autonomous purkinje cell degeneration and displays proteolytic cleavage in ataxic transgenic mice. *J. Neurosci.* **22**, 4897–4905 (2002).
36. Adachi, H. *et al.* Transgenic mice with an expanded CAG repeat controlled by the human AR promoter show polyglutamine nuclear inclusions and neuronal dysfunction without neuronal cell death. *Hum. Mol. Genet.* **10**, 1039–1048 (2001).
37. Terao, S. *et al.* Age-related changes in human spinal ventral horn cells with special reference to the loss of small neurons in the intermediate zone: a quantitative analysis. *Acta Neuropathol. (Berl.)* **92**, 109–114 (1996).